



Delft University of Technology

Effect of ground copper slag on the fresh properties of 3d printed cementitious composites

Nieświec, Martyna; Chajec, Adrian; Šavija, Branko

DOI

[10.1038/s41598-025-02996-8](https://doi.org/10.1038/s41598-025-02996-8)

Publication date

2025

Document Version

Final published version

Published in

Scientific Reports

Citation (APA)

Nieświec, M., Chajec, A., & Šavija, B. (2025). Effect of ground copper slag on the fresh properties of 3d printed cementitious composites. *Scientific Reports*, *15*(1), Article 18117. <https://doi.org/10.1038/s41598-025-02996-8>

Important note

To cite this publication, please use the final published version (if applicable). Please check the document version above.

Copyright

Other than for strictly personal use, it is not permitted to download, forward or distribute the text or part of it, without the consent of the author(s) and/or copyright holder(s), unless the work is under an open content license such as Creative Commons.

Takedown policy

Please contact us and provide details if you believe this document breaches copyrights. We will remove access to the work immediately and investigate your claim.



OPEN Effect of ground copper slag on the fresh properties of 3d printed cementitious composites

Martyna Nieświec^{1✉}, Adrian Chajec¹ & Branko Šavija²

3D printing is becoming increasingly popular in the construction sector. 3D printing offers the potential to reduce costs, construction time and construction waste. However, due to its high cement content, 3D printable concrete more expensive to produce. The article includes a brief literature survey on the possibility of using cement and aggregate substitutes in concrete mixtures and their impact on fresh composite properties and identifies a research gap. Herein, we propose the use of waste copper slag as a replacement for cement in 3D printable concrete. We examine the effect of replacing cement with copper slag at 5 and 10% on fresh properties of cementitious mortar. The results show that copper slag improves the workability of the mixture and lowers the design yield strength up to 44%, thereby facilitating printing. Even 30% higher fresh compressive strengths were also obtained, which suggest that the buildability of mortars containing copper slag will be improved.

Keywords 3D printable mortar, Copper slag, Sustainability, Fresh state compressive strength, Workability, Slug test

As concrete is the most widely used building material, the construction industry is being forced to develop and adopt more efficient and sustainable strategies of development and technologies to meet social, environmental and economic needs. A hopeful solution is 3D printing technology. Although 3D printable concrete is not yet very popular, it can be a very good economical and sustainable construction solution. 3D concrete printing allows the mixture to be laid in layers, without the use of formwork, with a high degree of accuracy. Its advantages include manufacturing speed and freedom of design. On the other hand, the challenge is to properly adjust the ingredients to achieve the right rheological properties and shrinkage of the hardened composite due to its high cement content. A major difference compared to cast concrete is that 3D printing concrete exhibits significant anisotropy: its mechanical properties depend on the direction of loading with respect to the arrangement of printed layers¹. Furthermore, 3D printable concretes typically contain higher amounts of cement compared to cast concrete and require access to expensive equipment². Before the technology can reach its full potential in the construction industry, gaps in research, cost analysis, socio-economic impact and lack of regulations must be filled³.

3D concrete printing has been shown to have many benefits. Batikha et al.⁴ compared the construction duration, cost and CO₂ emissions of constructing a two-story building using 3D printable concrete, prefabricated modular construction, monolithic reinforced concrete construction, cold-formed steel and hot-rolled steel. Making a structure from modular prefabricated construction takes the shortest construction duration but it is characterized by about 30% higher construction weight. This research shows that 3d printable concrete is the most sustainable solution next to cold-formed steel. It is characterized by lower cost and CO₂ emissions compared to other solutions. Similar conclusions were reached by Weng et al.⁵ who compared the cost, environmental impact and productivity of making a bathroom set with dimensions of 1.62 × 1.5 × 2.80 (length, width, height) meters using 3D printing and precast techniques. Material consumption, electricity expenditure, labor cost/efficiency and installation cycle were compared. The results show that the 3D printable component provides a reduction in total cost by more than 20%, and a reduction of CO₂ emissions and electricity consumption by more than 80%. It also allows the component to be made with lower weight. Paul et al.⁶ found that about half of construction costs are formwork costs, which are minimized using 3D printing technology. Since there is no need to prepare the formwork, construction time is also reduced.

Despite the many demonstrated benefits, one of the main drawbacks of 3D printing is the high binder content, which is up to twice that of conventional concrete⁷. Good material selection is an important parameter

¹Department of Materials Engineering and Construction Processes, Wrocław University of Science and Technology, Wybrzeże Wyspiańskiego 27, Wrocław 50-370, Poland. ²Faculty of Civil Engineering and Geosciences, Delft University of Technology, Stevinweg 1, Delft 2628 CN, The Netherlands. ✉email: martyna.nieswiec@pwr.edu.pl

to obtaining the desired print parameters and the finished composite. The choice of aggregate depends largely on the characteristics of the printer used. If the nozzle is small, it is not possible to use coarse aggregate. Various chemical admixtures are used to ensure that the mixture is printable, including admixtures that reduce the amount of water, modify viscosity, air content and admixtures that control the setting time⁸. Comparison of the composition of mixtures of different types and 3D printable concrete is shown in Fig. 1.

In addition to the higher amount of binder, a much lower w/b ratio is evident, especially in comparison to self-compacting and conventional concrete. With such a large difference in the amount of binder, replacing cement with more sustainable alternatives is crucial for reducing the environmental impact of 3D printable concrete.

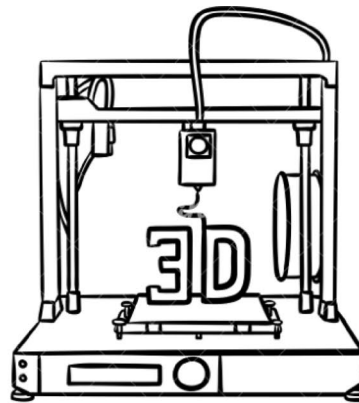
In concretes for 3D printing, the rheology of the mixture is crucial. Concrete suitable for 3D printing is often characterized by the Bingham model¹³ (see Eq. (1)), according to which the shear stress (τ) is closely related to the yield stress (τ_0), plastic viscosity (μ) and shear rate ($\dot{\gamma}$).

$$\tau = \tau_0 + \mu \dot{\gamma} \tag{1}$$

Three-dimensionally printed concrete flows when a certain shear stress is applied to it. Static flow stress is the peak shear stress required to initiate flow in static concrete. Dynamic flow stress is the shear stress required to maintain flow¹⁴. Over time, the static flow stress of a fresh concrete mixture increases due to intermolecular interaction and the initiation of cement hydration, a process called structuration¹⁵. Dynamic yield strength and plastic viscosity affect the pumping and extrusion stages of concrete, while static yield strength, thixotropy and rate of structuring define shape retention and buildability after extrusion¹⁶.

Advantages

- no formwork
- high degree of accuracy
- freedom of design
- high performance
- pace of work
- less labourer workers



Disadvantages

- design complications
- cost of the printer
- skilled personnel
- **high cement content**

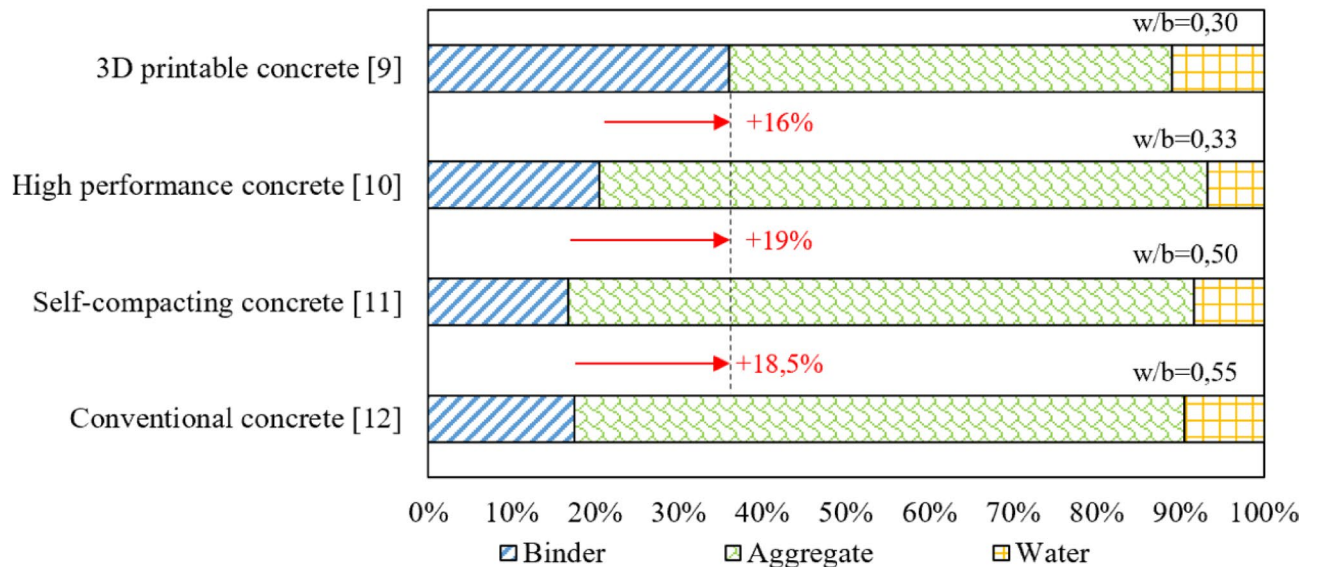


Fig. 1. Advantages and disadvantages of 3D printing [image generated from canva.com (free license), graph created in MS Excel for Microsoft 365 MSO version 2501 compilation 16.0.18429.20132 by Martyna Niesiewicz (the academic license of the Wrocław University of Science and Technology, license ID: EWW_91b69d94-d411-414f-be6e-34e2cd09b08b_4a5b0442d0746fa702)]

Reducing CO₂ emissions related to concrete production is important for society. One solution is to use a variety of waste materials as replacements for cement. In the Polish industry, it is worth focusing on the utilization of copper slag, of which as many as one million tons are produced annually in Poland alone. Poland is among the top copper-producing countries and has extensive resources of copper slag. For this reason, Polish scientists should focus on developing the field of research using post-copper slag.

The use of copper slag in cement composites has been studied for years. Manjunatha et al.¹⁷ observed that it can be used as a replacement for sand in concrete up to 60% without affecting the properties of fresh concrete and hardened composites. Gopalakrishnan et al.¹⁸ replaced cement with slag and got an improvement in properties of up to 30% replacement.

Copper slag consists mainly of Fe₂O₃ and SiO₂. We can also note the high SiO₂ content in fly ash, which according to the literature is the most common replacement for cement in concrete for 3D printing, and blast furnace slag (Table 1). It has significantly less CaO than other materials however the amount of Al₂O₃ is similar to cement. The significant amount of Fe₂O₃ distinguishes it from other materials, making it a material with high hardness.

It is worth noting that, to the best of the authors' knowledge, the replacement of cement with copper slag in 3D printing compounds has not been studied. There are some isolated works in which fine aggregate is substituted, however, there is a lack of works on the topics covered in the articles. The authors of this paper claim that the use of copper slag in 3D printing compounds can positively affect their properties, and most importantly, the environmental and economic aspects. To verify this, a flow table test and unconfined uniaxial compression test of cementitious mortars with copper slag were performed. Further research into the use of copper slag in 3D printing will help fill the research gap and may be useful not only in environmental terms but also in improving the properties of the mixture.

Designing a concrete mix for printing is an iterative process verified by the printing process. Printable concrete mixes typically have low dynamic yield strength for good extrusion, but have high thixotropic behavior after extrusion, increasing the static yield strength, allowing the concrete to hold its own weight and the weight of subsequent printed layers⁹. In addition to choosing the right materials, printing parameters such as printing speed and nozzle width are important. The amount of extruded material and the width of the print line depend on the printing speed, so for a given nozzle width, it is necessary to find the optimal speed that does not cause cracks in the material and creates a good suitable print path²². The shape of the nozzles affects printability and the shape and fluidity of the mixture. For nozzles with a round shape, the penetration rate increases slightly. The reason for this is the lower flatness of the previous layer, which is arranged as a concave shape²³.

Due to the large amount of cement, supplementary cementitious materials are used. Among the most popular are fly ash, metakaolin and silica fume²⁴. Table 2 collects and shows the impact of several of the most used cement substitutes. The impact of a single ingredient is listed, although many are often used at once to improve properties.

A review of the literature shows that supplementary cementitious materials, such as for example fly ash or metakaolin, are widely used to design compounds for 3D printing. Including them improves or does not significantly deteriorate their properties.

Among the brief literature search performed, no copper slag was found as a supplementary cementitious material. Ma et al.⁴¹ replaced fine aggregated up to 50% with copper tailing. An increase in flowability and a decrease in buildability were observed as the degree of replacement increased. The optimal replacement was found to be 30%. Similar conclusions were reached using copper slag in conventional concretes. Li et al.⁴² replaced aggregate entirely with iron and copper waste. A material with good workability, fluidity and controlled setting time was obtained, allowing 3D printing. In addition, radioactivity and toxicity were tested and the material was found to be safe for human use.

From the research described above, the use of 3D printing in the construction sector shows promise. The main CO₂ emissions come from cement production, and the cost comes from the use of cement and the 3D-printer. For this reason, it is important to find a waste material that can be used to partially replace cement and further reduce the cost and CO₂ emissions compared to conventional concrete. Replacing even a few percent of cement could be crucial not only for the properties of composites, but also for CO₂ emissions, especially if 3D printing becomes widespread in the industry.

The use of copper slag in cement composites has already been studied in many publications⁴³. The present work indicates its new application in mixtures for 3D printing. Such a solution has not been analyzed so far, so

	Copper slag ¹⁹	Blast furnace slag ²⁰	Fly ash ²¹	CEM I 42.5 R (used in this study)
SiO ₂	30.53	38.07	41.94	18.3
Al ₂ O ₃	2.80	11.82	33.27	4.7
Fe ₂ O ₃ /FeO	57.82	0.44	10.22	2.8
CaO	1.60	38.28	5.78	67.2
MgO	1.48	5.93	-	2.5
SO ₃	1.59	1.88	5.48	2.6
K ₂ O	0.71	0.69	1.05	1.8
Others	Up to 100%			

Table 1. Chemical composition of copper slag and different materials.

Number of publications*	Supplementary cementitious materials (SCM)	Effect	References
50	Fly ash	Cement replacement results in the ability to achieve the desired flow and workability while maintaining adequate strength properties. Fly ash can help reduce shrinkage.	[26], [27], [28], [29], [30].
31	Silica fume	The addition of silica fume increased the stiffness of the mixtures and the rate of strength development. Improved also the yield stress and maintained the desired viscosity of the concrete mix. Replacing cement with up to 16% silica fume in 3D printing foam concrete resulted in an increase in density, yield strength, viscosity and buildability of the mixture.	[26], [31], [32], [33]
13	Metakaolin	Use of metakaolin improves thixotropy and shape stability but worsens workability and setting time. An increase in static yield strength were also observed. The use of MTK did not change the strengths	[34], [35], [36], [37]
7	Limestone powder	The inclusion of limestone powder reduces liquidity loss and yield stress and worsens the buildability. Increasing LP content results in an increased extrudability and a decrease in buildability.	[38], [39]
4	Nano silica	The addition of nanosilica improves yield stress, thixotropy and buildability but worsen setting time.	[40], [41.]
0	Copper slag	NO DATA	NO DATA

Table 2. The effect of replacing cement with popular supplementary cementitious materials on the fresh properties of 3D printable mixtures.

*ScienceDirect ,3D printed concrete + SCM” in title, abstract or keyword, date: 16.09.2024.

the article is a valuable source of information. Research on the use of copper slag as a replacement for cement in cement composites fills a huge research gap.

Materials and methods

Materials and mixes

The reference mortars were designed as mix of Portland cement CEM I 42,5R (Odra S.A., Poland), quartz sand (AXTON, Poland, $d_{max}=2$ mm) and tap water. The superplasticizer was used in all tested mixes to reduce needed amount of water (ATLAS Sp. z o. o., Poland).

Copper slag from a Polish copper mine was used in the study as replacement of cement. Before use, the copper slag was ground (Fig. 2) for 1 h in a ball mill. Longer grinding does not significantly improve grain size and uses more electricity. Grinding efficiency (E) was defined as the ratio of particles under 0.25 mm to electricity consumption (Fig. 3a). Steel balls with diameters of 2 and 4 cm were used as grinding media. The ratio of steel balls to copper slag was 1:1 by volume and mill was filled of 30% without grinding accelerators based on the literature⁴⁴. After grinding, the copper slag was sieved, rejecting particles above 0.25 mm (Fig. 3b).

To check the reactivity of the copper slag, the R^3 test was performed as recommended by RILEM⁴⁵. A paste was made with 10 g of copper slag, 30 g of calcium hydroxide, 5 g of calcium carbonate and 54 g of potassium solution. The paste samples were cured for 7 days in containers at 40 °C. Then the samples were crushed, sieved through a 2 mm sieve and dried again for 24 h. The dried samples were dehydrated at 350 °C and the bound water was calculated according to Eq. (2), where w_o is the total mass of dried paste and laboratory pot, w_h is the total mass of the hydrated paste and laboratory pot and w_c is the total mass of the empty laboratory pot.

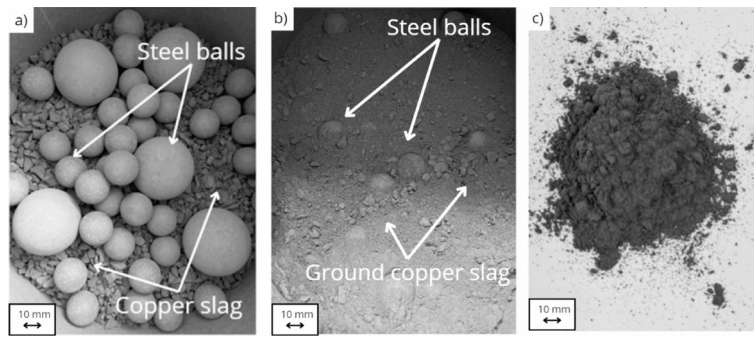


Fig. 2. Copper slag and steel balls in fill mil **a)** before grinding, **b)** ground copper slag, **c)** copper slag after grinding and sieving [author of the photos: Martyna Nieświec]

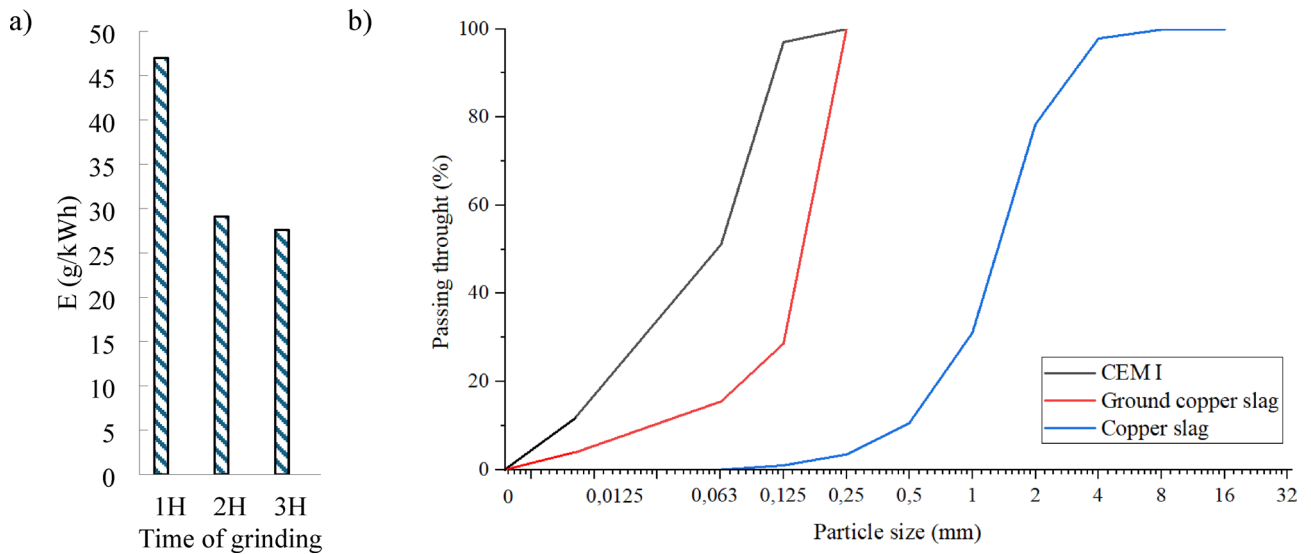


Fig. 3. Impact of copper slag grinding on: **a)** grinding efficiency; **b)** particle size distribution. [graphs created in MS Excel for Microsoft 365 MSO version 2501 compilation 16.0.18429.20132 by Martyna Nieświec (the academic license of the Wrocław University of Science and Technology (license ID: EWW_91b69d94-d411-414f-be6e-34e2cd09b08b_4a5b0442d0746fa702)].

$$H_2O_{bound,dried} = \frac{w_0 - w_h}{w_0 - w_c} \left(\frac{g}{100 \text{ g dried paste}} \right) \tag{2}$$

As a reference for evaluating and interpreting the results of the R³ test, a compressive strength test was performed according to the standard⁴⁶, in which 30% of the cement was replaced with copper slag (CS30). This type of specimen was used only to check the compressive strength for interpreting the results of the R³ test. R_{CS,relative} was calculated according to Eq. (3), where R_{CS} is the compressive strength of the mortars containing copper slag (the average from 6 testes) and R_{CM} is a compressive strength of the reference mortar without copper slag.

$$R_{SC,relative} = \frac{R_{CS} - R_{CM}}{R_{CM}} \times 100\% \tag{3}$$

In addition, two mortars were prepared in which cement was replaced by ground copper slag in amounts of 5 (CS5) and 10 (CS10) %. The w/b ratio was constant: w/b=0.2. The mixture compositions are presented in Table 3.

The mixing is performed at temperature 20 ± 2 °C and relative humidity above 50% using a mechanical mixer according to the standard PN-EN 196-1:2016-07 for 150 s in two stages⁴⁶. First, all ingredients were weighted (solids to the nearest 2 g and water to the nearest 1 ml). Then, cement and water were placed in the mixer and mixed at slow speed for 30 s. Next, aggregate was added, and the mixer was turned on high speed. After 30 s, the mixer was stopped for 90 s (to scratch mortars from container walls) and then mixed at high speed for 60 s. After that, the mixes were used in different tests.

Ingredient	Research series			
	REF (kg/m ³)	CS5 (kg/m ³)	CS10 (kg/m ³)	CS30 (kg/m ³)**
Portland cement CEM I	1278.95	1215.00	1151.05	895.27
Grounded copper slag	0	63.95	127.89	383.67
Quartz sand	639.47	639.47	639.47	639.47
Tap water	255.79	255.79	255.79	255.79
Superplasticizer	12.79 /6.39*	12.79 /6.39*	12.79 /6.39*	12.79

Table 3. Mixes used in research. *Unconfined uniaxial compressive test. **Only as a reference for evaluating and interpreting the results of the R³ test.

Flow table test

The mixture flowability was determined using a flow table test according to standard PN-EN 1015-3⁴⁷. A conical ring was placed on the disc and filled with fresh material in two layers. Each layer was compacted by poking 10 times. The excess material was removed from the top of the ring and the surface was leveled. After 15 s, the ring was removed, and the table was shaken 15 times (about once per second). The diameter in two perpendicular directions (*a* and *b*) was measured, and the diameter of the flow was calculated using Eq. (4). The spread of the mixture was determined as an average of 3 measurements.

$$r_m = \frac{(a + b)}{2} \text{ (mm)} \quad (4)$$

Yield stress measurement – slug test

The yield strength of 3d printable mixtures was measured using the slug test according to RILEM TC PFC⁴⁸. Immediately after the mixing, the fresh material was placed in the printer's container. The printer, whose plunger is moved by air pressure (0,05 MPa), was used for testing. A previously weighed bucket (*m_b*) on a scale was placed under the printer nozzle with a diameter 6 mm at a distance 30 cm. After placing the mixture in the feeder (in two layers, compacted by 10 beats on the table), recording video was started and the mixture was allowed to flow freely at a fixed air pressure of 0.5 MPa. The cross-sectional area of the nozzle (*S*) was determined, shape category of the slugs was recorded with a phone (iPhone 13, 12 MPx, 30 frames per second, 4 K recording). The weight of slugs was measured with a scaled and the average (*m_s*) was calculated. The test was conducted in a room with a temperature of 20 ± 2 °C and a humidity of 50% making a minimum of 15 slugs for each mixture. Figure 4 shows the experimental setup. The yield stress was calculated using Eq. (5). The average of 3 measurements was considered as the result. Weights were measured to the nearest 0.1 g, lengths to 0.1 mm.

$$\tau = 100 \cdot \frac{m_s}{\sqrt{3} \cdot S} \text{ (MPa)} \quad (5)$$

Fresh state strength

To check the relationship between deformation and mortar strength at the very early age, a fresh state compression test of cementitious mortar was performed. After mixing, the mixture was placed and compacted in two layers in demountable cylindrical molds with a diameter (*A*) of 5 cm and a height (*L*) of 10 cm and noted the time. Before laying the mixture, the molds were lined with foil. After casting, the samples were set aside. After the intended time (5, 15, 30 and 45 minutes), the sample was carefully placed in the test place (Fig. 5a), the mold was removed (Fig. 5b), and then the films were carefully removed. Then the test was started (Fig. 5c), with a constant speed of 42 mm/min, and the force (*F*) and vertical displacement (*l*) were recorded.

The stress (*f*) was calculated using Eq. (6) and strain (*ε*) using Eq. (7). Each test was repeated 3 times. A constant cross-sectional area of the sample was assumed for the calculations, i.e. not considering the deformed shape during the deformation.

$$f = \frac{F}{(A/A^2)4} \text{ (kPa)} \quad (6)$$

$$\epsilon = \frac{l}{L} \text{ (-)} \quad (7)$$

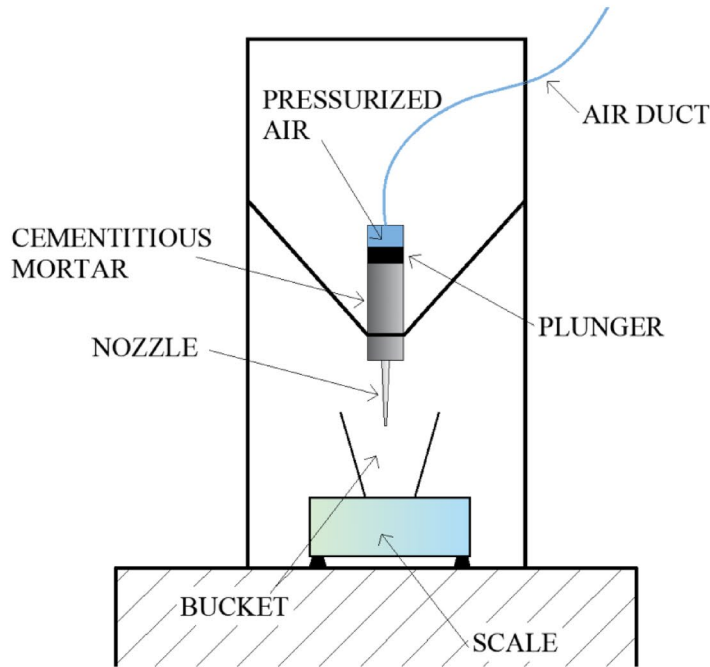
Results

R³ test

R³ test results showed a bound water amount of 1.32 g/100 g dried paste (Fig. 6). This is a very low value suggesting that the copper slag in this case acts only as a filler material, and not a binder. For reactive materials, this value is several times higher (from 5 to even 12%)⁴⁵. A lower compressive strength was observed after 3 and 7 days for mortars containing 30% copper slag, confirming the above Hypothesis. Both after 3 and 7 days the compressive strength decreased by almost 30%.

This can also be confirmed by the studies of Edwin et al.⁴⁹, who concluded that the use of copper slag has a limited effect on the heat generation during hydration of the cement paste. They also demonstrated the low pozzolanic activity of this material.

a)



b)



Fig. 4. Slug test stand a) Schematic view of the experimental place [image created in AutoCAD 2023 version T.53.0.0 by Martyna Nieświec (the academic license of the Wrocław University of Science and Technology, license ID: 68224553969032)]; b) photo of experimental place [author of photo: Martyna Nieświec].

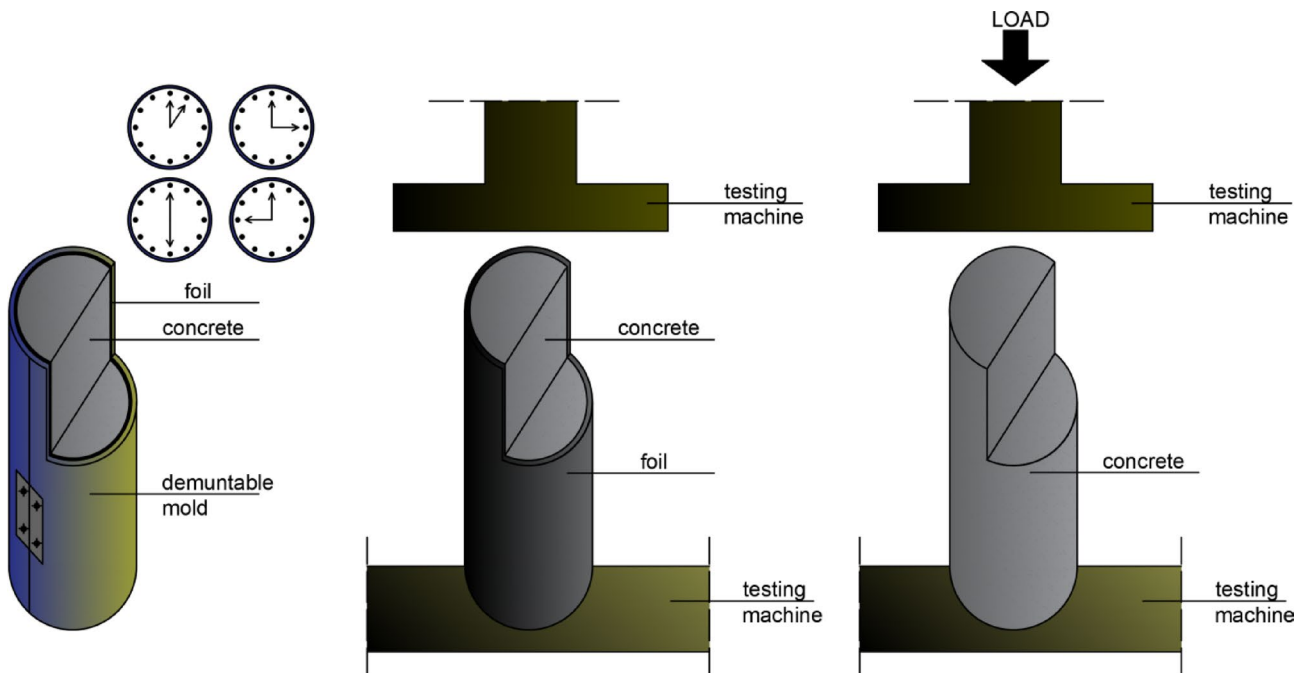


Fig. 5. Performing the test: sample in demountable form, mold remover and testing [all created in AutoCAD 2023 version T.53.0.0 by Martyna Nieświec (the academic license of the Wrocław University of Science and Technology, license ID: 68224553969032)]

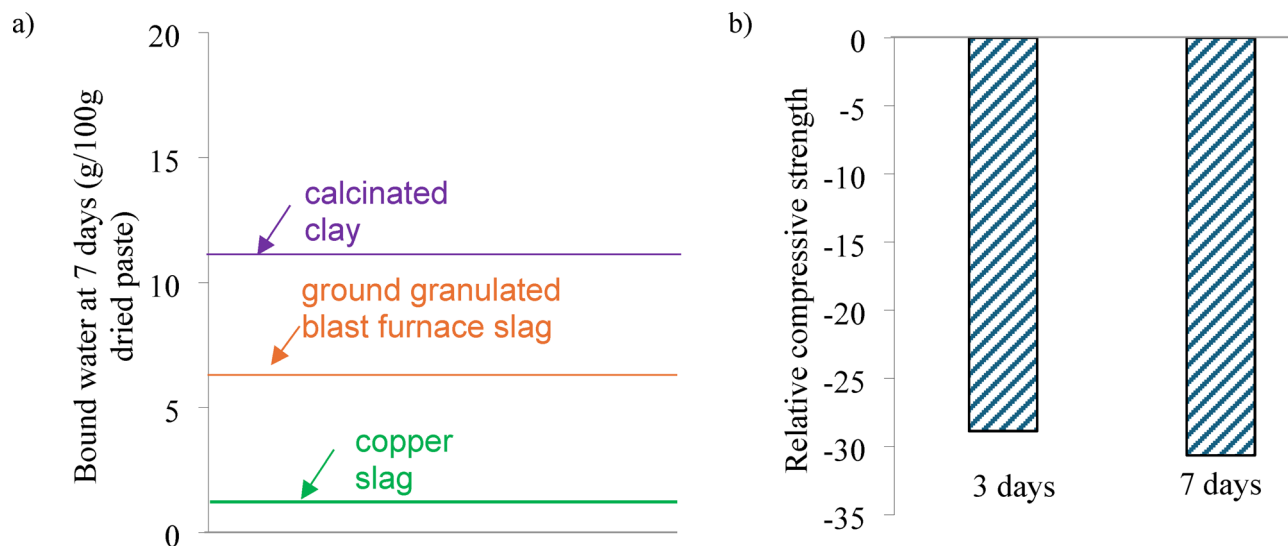


Fig. 6. Results of R^3 test: (a) bound water at 7 days, (b) relative compressive strength after 3 and 7 days [based on own research and^{45,50}, created in MS Excel for Microsoft 365 MSO version 2501 compilation 16.0.18429.20132 by Martyna Nieświec (the academic license of the Wrocław University of Science and Technology, license ID: EWW_91b69d94-d411-414f-be6e-34e2cd09b08b_4a5b0442d0746fa702)]



Fig. 7. Spreading of cementitious mortars [author of the photos: Martyna Nieświec].

With such a high replacement of cement, it is difficult to expect an increase in strength. Afshoon and Sharifi⁵¹ showed that replacing cement up to 10% by copper slag improved the compressive strength of mortars, while higher replacement levels resulted in lower strength.

Slump flow and slug test

Replacing cement with copper slag leads to improved workability and affects the consistency of the mixture. The slump flow increased as the amount of copper slag increased: by 12% for CS5 and by 24% for CS10 (Fig. 7). The results obtained are in line with those obtained earlier replacing cement with slag in SCC concretes^{51,52}. The slump spread has been shown to be a good indicator of concrete printability: Tay et al.¹³ showed that mixtures with a spread diameter lower than 130 mm are too stiff and cannot be extruded smoothly while those with a diameter higher than 210 mm are too fluid and do not allow consistent printing. Thus, it can be assumed that the best printable will be a mixture of CS5.

Replacing cement with copper slag results in a decrease in yield strength, as shown in Fig. 8. Replacing cement with 5% copper slag reduces calculated yield strength by 23%, while replacing 10% cement by copper slag reduces it by 44%. Concrete with a higher viscosity and a lower yield strength result in higher plasticity and better workability⁵³.

As the copper slag content increased, the length of the slug decreased (Fig. 9). The photo below shows a selection of isolated from video slugs. In general, the length of slugs from the CS5 mixture was almost 30%

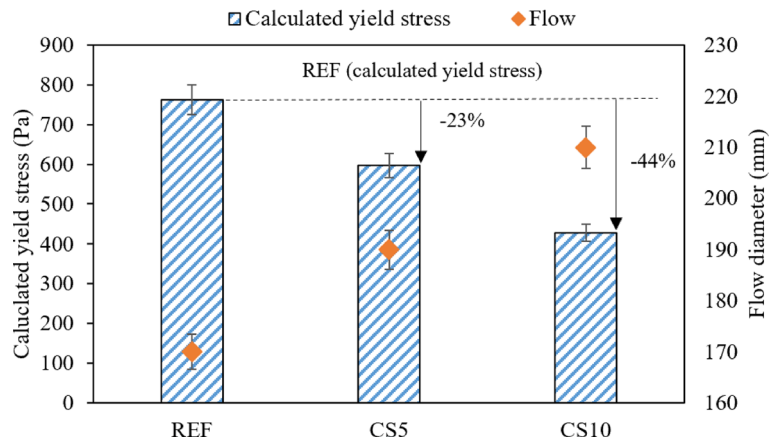


Fig. 8. Calculated yield stress and flow diameter of the tested cementitious mortars [created in MS Excel for Microsoft 365 MSO version 2501 compilation 16.0.18429.20132 by Martyna Nieświec (the academic license of the Wrocław University of Science and Technology, license ID: EWW_91b69d94-d411-414f-be6e-34e2cd09b08b_4a5b0442d0746fa702)]

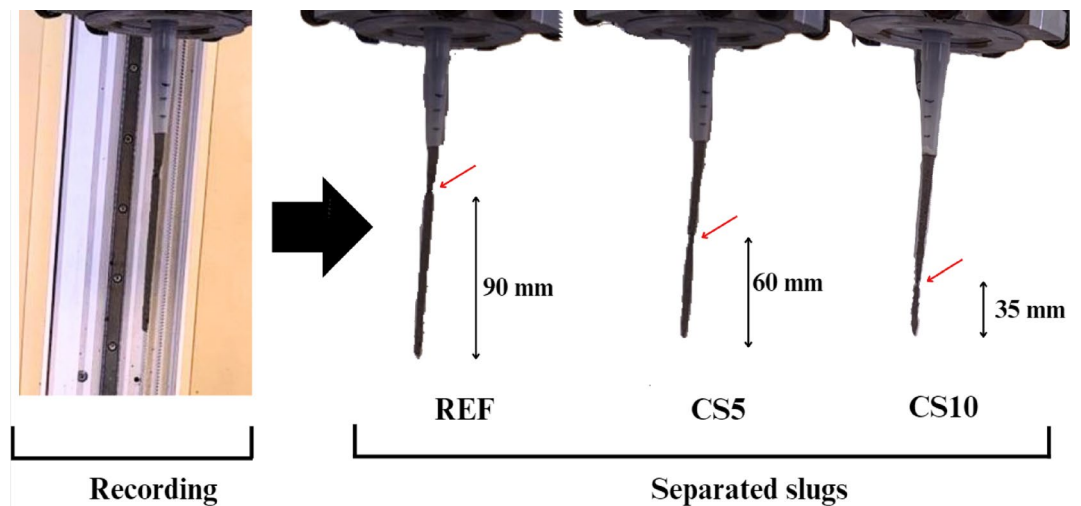


Fig. 9. Registered types of slugs in the slug test without and with copper slag [author of the photos: Martyna Nieświec, created in AutoCAD 2023 version T.53.0.0 by Martyna Nieświec (the academic license of the Wrocław University of Science and Technology, license ID: 68224553969032)]

shorter than the REF mixture, and the CS10 mixture more than doubled. Slugs REF and CS5 display constant cross section areas, in turn CS10 slug is deformed and does not show a constant cross section area. Slugs can be classified as plastic for REF, visco-plastic for CS5 and viscous for CS10⁴⁸. The longest slugs were obtained for the reference mixture (REF).

Fresh state strength

The results of fresh compressive strength for all series are shown in Fig. 10. For all testing times, the CS5 mixes have less displacement than the REF mix and more than the CS10 mix at the same force. This means higher stiffness. For all testing times, the destruction of samples containing 5% copper slag occurred at a higher force than the reference sample. The increase in stiffness is more pronounced at 10% copper slag. Differences in the force-displacement relationship increase with time for cementitious mortars with copper slag.

The failure mechanisms were similar for all mixtures (Fig. 11), only the forces at which they occurred differed. After 5 min, the highest deformation is seen at the bottom of the cylinder. After 15 min, the deformation at the bottom decreases and moves to the top of the cylinder after 30 min. After 45 min, the deformation decreases, and diagonal cracks in the sample become visible. At earlier ages, the mixture is less stiff and deforms under pressure and its own weight. As it ages, it becomes stiffer and is able to take more load with less deformation.

Replacing cement with copper slag increases the fresh state strength (Fig. 12). The maximum destructive force was obtained after 45 min and was 52 N for REF mix, 63.5 N for CS5 and 67 N for CS10 mix. For each test

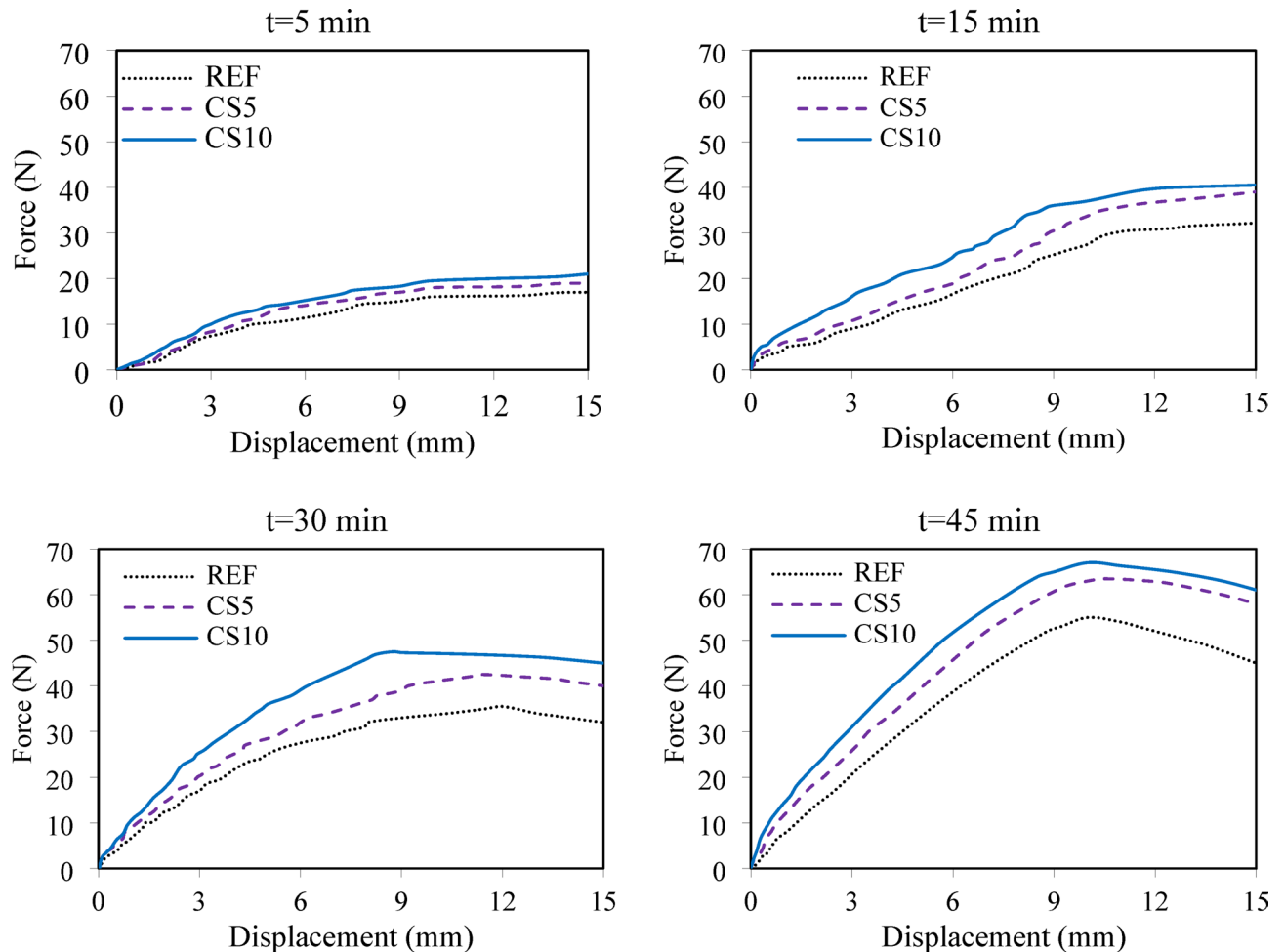


Fig. 10. The relationship between force and displacement for fresh compression test after 5, 15, 30 and 45 min [created in MS Excel for Microsoft 365 MSO version 2501 compilation 16.0.18429.20132 by Martyna Nieświec (the academic license of the Wrocław University of Science and Technology, license ID: EWW_91b69d94-d411-414f-be6e-34e2cd09b08b_4a5b0442d0746fa702)]

time, the displacement of the mixes with copper slag was less than that of the reference mortar. The graph for the reference sample is the most flattened, indicating that less stiffness. The destructive force of the sample increases with the addition of copper slag. The increase in stress is 12% for CS5 and 15% for CS10 after 5 min, while after 45 min it is 21% for CS5 and 42% for CS10. This can be influenced by the irregular shape of the slag grains. To confirm this, further testing should be done and verified with the buildability of the mix after printing.

As it has been shown that copper slag acts as a filler material, it can be assumed that the improved green strength is a result of improved packing. It is well established that improved particle packing results in higher buildability, provided that the material is printable⁵⁴.

In an elastic material, the slope (stress-strain) of the graph corresponds to Young's modulus. There amount of elastic deformation at the very early age is limited. However, with certain limitations it is possible to use this parameter as Young's modulus⁵⁵. In the literature it takes the term as apparent Young's modulus⁵⁵, elastic modulus⁵⁶ or stiffness modulus⁵⁷. Figure 12 shows that the apparent Young's modulus, defined as the slope of the graphs, is higher for the material containing copper slag. From the peak stress values, it is possible to determine the maximum stress that the sample can withstand, i.e. its green strength. The compressive strength is more than 15% higher for CS5 and nearly 30% higher for CS10 compared to the sample REF.

An important aspect of the research conducted was to determine the role performed by the copper slag in the tested cementitious composite. It was verified that it does not act as an additional reactive material and is only a filler. The glassy surface of the slag has a positive effect on its workability. In addition, a lower yield strength was obtained. This results in the need to overcome lower force needed to extrusion. Both aspects can have a positive impact on the subsequent printability of the composites. However, it should be taken into account that a higher percentage of cement replacement with copper slag may lead to the mixture flowing too quickly, making it impossible to print. The higher early compressive strength may be due to better compaction of the composite. As a result, we can expect better buildability of the composite (Fig. 13). The information obtained provides many opportunities for future research.

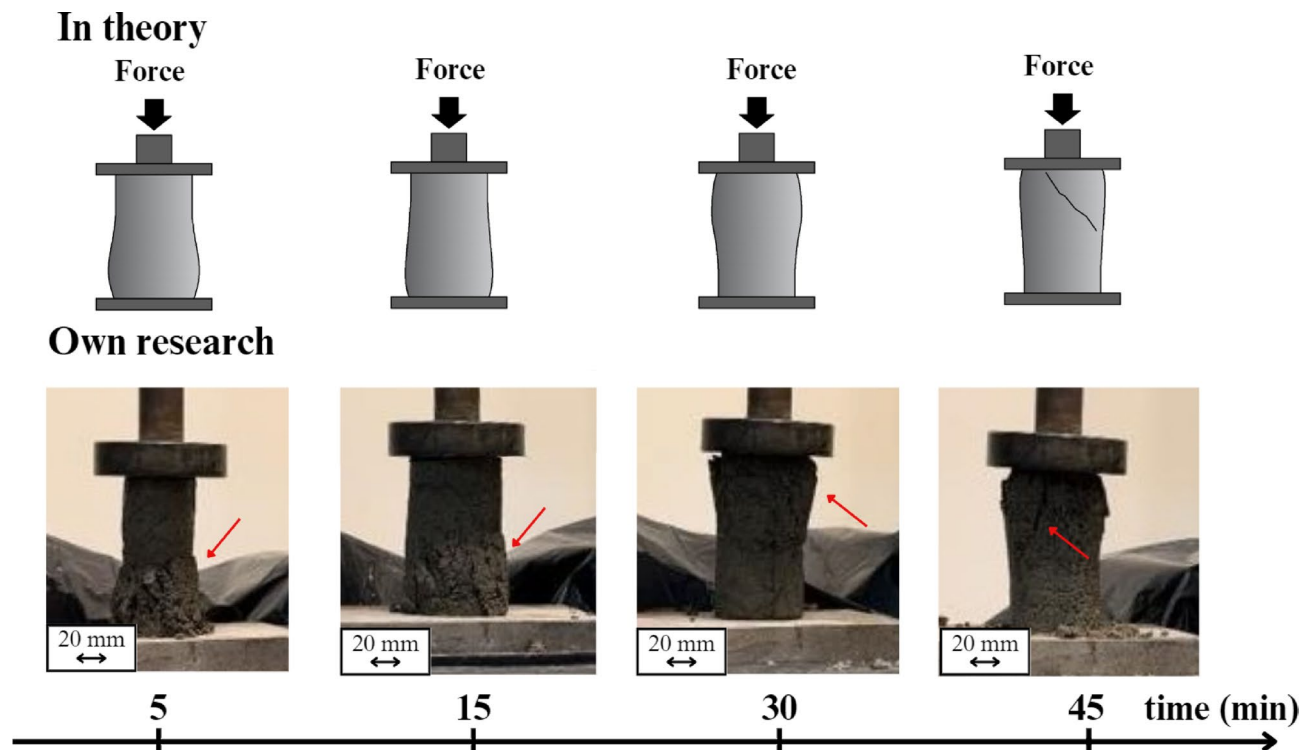


Fig. 11. Damage mechanism of cylindrical specimens in fresh compressive strength test (photos for reference samples) [author of the photos: Martyna Nieświec, images created in AutoCAD 2023 version T.53.0.0 by Martyna Nieświec (the academic license of the Wrocław University of Science and Technology, license ID: 68224553969032)]

Replacing cement by ground copper slag not only improves the properties of cement composites but also has a positive impact on the environment by reducing CO₂ emissions.

Conclusions

The study investigated the effect of copper slag on the properties of composites for 3D printing. The work presented here is a source of information on the use of copper slag in cement composites. The following conclusions can be drawn from the presented work:

- The workability of cementitious composites is increased due to the slag glassy structure. Mixture slump flow increases by 24% when replacing cement by 10% and by 12% when replacing cement by 5%.
- The inclusion of slag causes a decrease in yield strength even by 44%, which can result in better printability of the composite due to lower frictional forces.
- Replacing cement with copper slag increases green compressive strength about 12% for CS5 and 15% for CS10 after 5 min, while after 45 min it is 21% for CS5 and 42% for CS10. The reason may be the irregular shape of the grains, but the results are not obvious, so further tests should be conducted and compared with the buildability of the mixture.
- The amount of bound water is only 1.32% while the strength of mortars after 3 and 7 days decreases by almost 30%. This means that the investigated copper slag functions only as a filler material. It has a positive effect on the filler effect, but it does not help the binding.

Future research direction

The authors of the paper also propose the directions for further research. Researchers should focus more extensively on the use of industrial waste and follow this research direction to further minimize the cost and environmental impact of 3D printing. The use of copper slag in concrete for 3D printing has not been sufficiently explored. It is necessary to study the remineralization properties of the fresh mixture and the hardened composite, and to find the optimal amount of copper slag addition taking into account not only the properties of the mixture, but also a safe amount⁵⁹. It will be useful to examination of copper slag of different origins and fractions, because the chemical composition of its depending on the method and place of production⁶⁰.

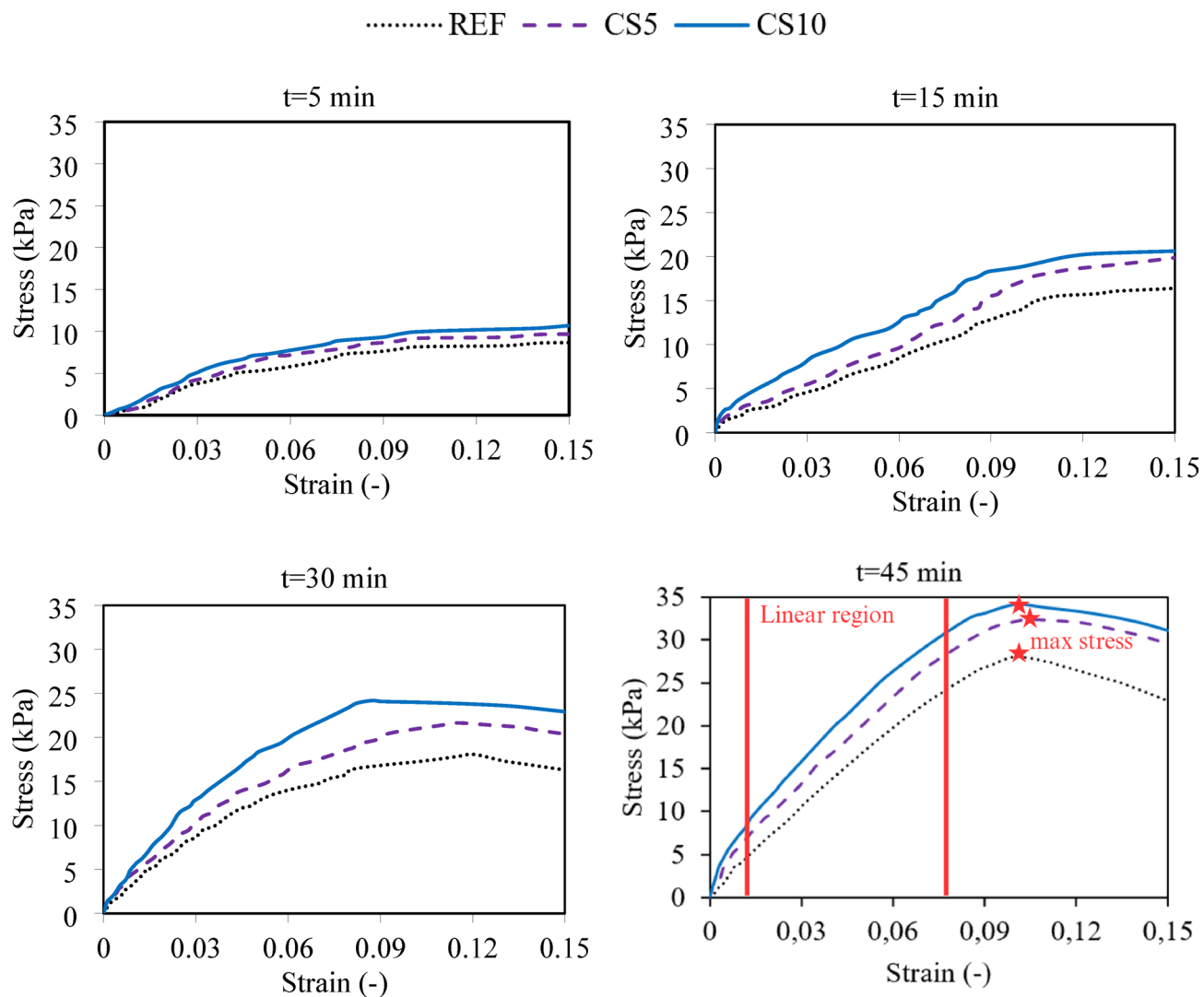


Fig. 12. The relationship between stress and strain for fresh compressive test [created in MS Excel for Microsoft 365 MSO version 2501 compilation 16.0.18429.20132 by Martyna Nieświec (the academic license of the Wrocław University of Science and Technology (license ID: EWW_91b69d94-d411-414f-be6e-34e2cd09b08b_4a5b0442d0746fa702)].

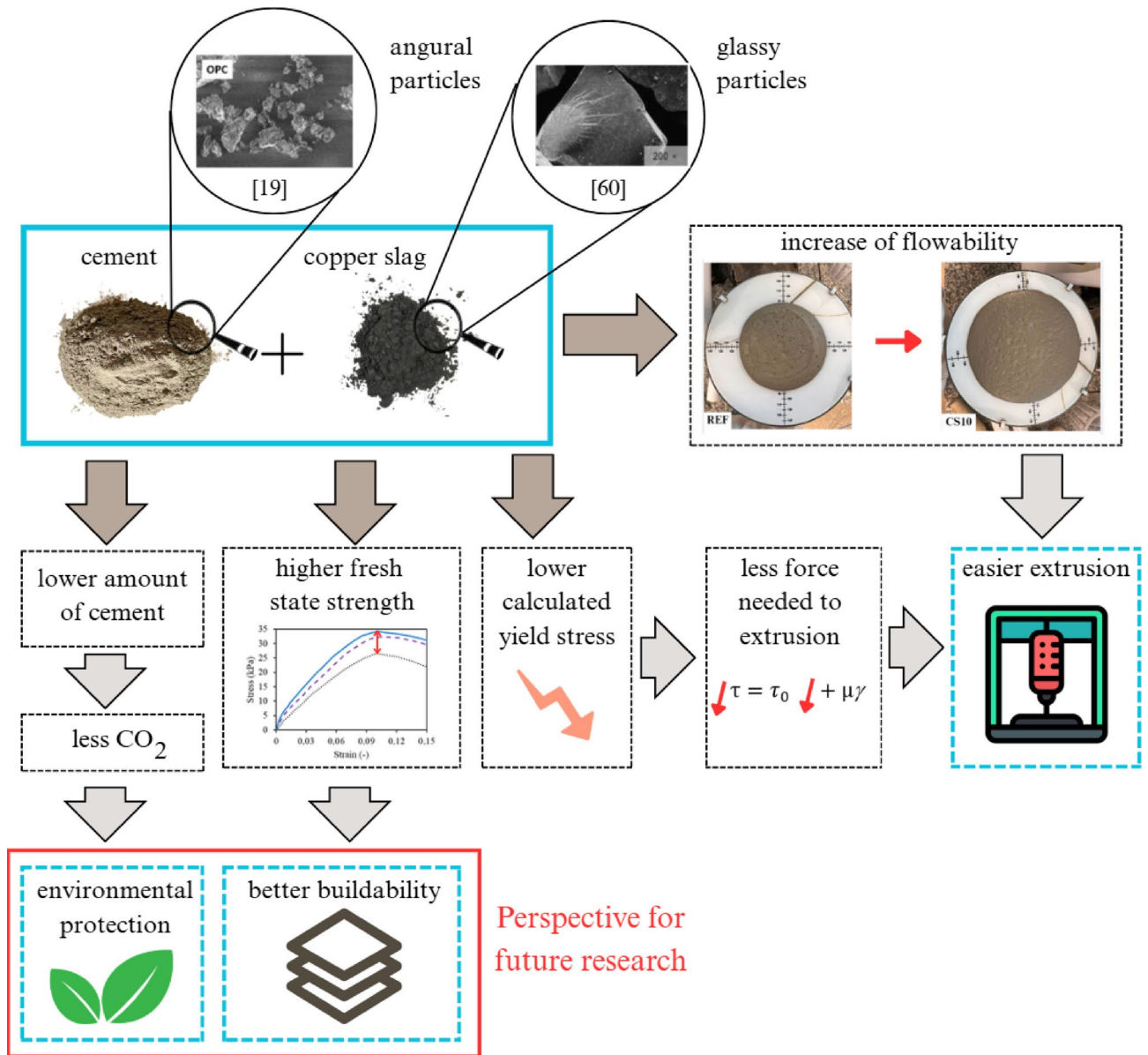


Fig. 13. The major relationships occurring due to replacement of cement with copper slag [SEM images from^{19,58} (according to the caption on the drawing), author of the photos: Martyna Nieświec, full graphic and other images created in canva.com by Martyna Nieświec (free license)]

Data availability

Data is provided within the manuscript.

Received: 28 January 2025; Accepted: 19 May 2025

Published online: 24 May 2025

References

- Liu, D., Zhang, Z., Zhang, X. & Chen, Z. 3D printing concrete structures: state of the art, challenges, and opportunities. *Constr. Build. Mater.* **405** <https://doi.org/10.1016/j.conbuildmat.2023.133364> (2023).
- Motalebi, A., Khondoker, M. A. H. & Kabir, G. A systematic review of life cycle assessments of 3D concrete printing. *Sustainable Oper. Computers.* **5**, 41–50. <https://doi.org/10.1016/j.susoc.2023.08.003> (2024).
- Akman, A. & Sadhu, A. Recent development of 3D-Printing technology in construction engineering. *Pract. Periodical Struct. Des. Constr.* **29** (1), 03123005. <https://doi.org/10.1061/PPSCFX.SCENG-1278> (2024).
- Batikha, M., Jotangia, R., Baaj, M. Y. & Mousleh, I. 3D concrete printing for sustainable and economical construction: A comparative study. *Autom. Constr.* **134** <https://doi.org/10.1016/j.autcon.2021.104087> (2022).
- Weng, Y. et al. Comparative economic, environmental and productivity assessment of a concrete bathroom unit fabricated through 3D printing and a precast approach. *J. Clean. Prod.* **261** <https://doi.org/10.1016/j.jclepro.2020.121245> (2020).

6. Paul, S. C., Tay, Y. W. D., Panda, B. & Tan, M. J. Fresh and hardened properties of 3D printable cementitious materials for Building and construction. *Archives Civil Mech. Eng.* **18**, 311–319. <https://doi.org/10.1016/j.acme.2017.02.008> (2018).
7. Mohan, M. K. et al. Performance criteria, environmental impact and cost assessment for 3D printable concrete mixtures. *Resour. Conserv. Recycl.* **181**, 106255. <https://doi.org/10.1016/j.resconrec.2022.106255> (2022).
8. Sahin, H. G. & Mardani, A. Assessment of materials, design parameters and some properties of 3D printing concrete mixtures; a state-of-the-art review. *Constr. Build. Mater.* **316**, 125865. <https://doi.org/10.1016/j.conbuildmat.2021.125865> (2022).
9. Rehman, A. U. & Kim, J. H. 3D concrete printing: A systematic review of rheology, mix designs, mechanical, microstructural, and durability characteristics. In: *Materials*, **14**, 3800 (2021). <https://doi.org/10.3390/ma14143800>
10. Soleymani, H. R. & Ismail, M. E. Comparing corrosion measurement methods to assess the corrosion activity of laboratory OPC and HPC concrete specimens. In: *Cement and concrete research* **34**, 11 : 2037–2044. (2004). <https://doi.org/10.1016/j.cemconres.2004.03.008>
11. Alyamac, K. E. & Ince, R. A preliminary concrete mix design for SCC with marble powders. *Constr. Build. Mater.* **23** (3), 1201–1210 (2009).
12. Silva, Y. F., Burbano-Garcia, C., Araya-Letelier, G. & Gonzalez, M. Short- and long-term experimental performance of concrete with copper slag: Mechanical and physical properties assessment. In: *Case Studies in Construction Materials* (2024). <https://doi.org/10.1016/j.cscm.2024.e03302>
13. Tay, Y. W. D., Qian, Y. & Tan, M. J. Printability region for 3D concrete printing using slump and slump flow test. *Compos. Part. B: Eng.* **174**, 106968. <https://doi.org/10.1016/j.compositesb.2019.106968> (2019).
14. Jayathilakage, R., Rajeev, P. & Sanjayan, J. Rheometry for concrete 3D printing: a review and an experimental comparison. In: *Buildings*, **12** (8), 1190 (2022). <https://doi.org/10.3390/buildings12081190>
15. Jayathilakage, R., Rajeev, P. & Sanjayan, J. Extrusion rheometer for 3D concrete printing. *Cem. Concr. Compos.* **121**, 104075. <https://doi.org/10.1016/j.cemconcomp.2021.104075> (2021).
16. Khoshnevis, B., Hwang, D., Yao, K. T. & Yeh, Z. Mega-scale fabrication by contour crafting. *Int. J. Ind. Syst. Eng.* **1** (3), 301–320. <https://doi.org/10.1504/IJISE.2006.009791> (2006).
17. Manjunatha, M., Reshma, T. V., Balaji, K. V. G. D., Bharath, A. & Tangadagi, R. B. The sustainable use of waste copper slag in concrete: An experimental research. In: *Materials Today: Proceedings*, **47**, 3645–3653. (2021). <https://doi.org/10.1016/j.matpr.2021.01.261>
18. Gopalakrishnan, R. & Nithyanantham, S. Microstructural, mechanical, and electrical properties of copper slag admixed cement mortar. *J. Building Eng.* **31** <https://doi.org/10.1016/j.jobe.2020.101375> (2020).
19. Sharma, R. & Khan, R. A. Sustainable use of copper slag in self compacting concrete containing supplementary cementitious materials. *J. Clean. Prod.* **151**, 179–192. <https://doi.org/10.1016/j.jclepro.2017.03.031> (2017).
20. Cheah, C. B., Liew, J. J., Le Ping, K. K., Siddique, R. & Tangchirapat, W. Properties of ternary blended cement containing ground granulated blast furnace slag and ground coal bottom Ash. *Constr. Build. Mater.* **315**, 125249. <https://doi.org/10.1016/j.conbuildmat.2021.125249> (20).
21. Ghanim, A. A., Rahman, F. U., Adil, W., Zeyad, A. M. & Magbool, H. M. Experimental investigation of industrial wastes in concrete: mechanical and microstructural evaluation of pumice powder and fly Ash in concrete. *Case Stud. Constr. Mater.* **18**, e01999. <https://doi.org/10.1016/j.cscm.2023.e01999> (2023).
22. Shakor, P., Nejadi, S., Sutjipto, S., Paul, G. & Gowripalan, N. Effects of deposition velocity in the presence/absence of E6-glass fibre on extrusion-based 3D printed mortar. *Additive Manuf.* **32**, 101069. <https://doi.org/10.1016/j.addma.2020.101069> (2020).
23. Shakor, P., Nejadi, S. & Paul, G. A study into the effect of different nozzle shapes and fibre-reinforcement in 3D printed mortar. In: *Materials*, **12**(10), 1708. (2019). <https://doi.org/10.3390/ma12101708>
24. Hou, S., Duan, Z., Xiao, J. & Ye, J. A review of 3D printed concrete: performance requirements, testing measurements and mix design. *Constr. Build. Mater.* **273**, 121745. <https://doi.org/10.1016/j.conbuildmat.2020.121745> (2021).
25. Panda, B. & Tan, M. J. Rheological behavior of high volume fly Ash mixtures containing micro silica for digital construction application. *Mater. Lett.* **237**, 348–351. <https://doi.org/10.1016/j.matlet.2018.11.131> (2019).
26. Ibrahim, A. & Kumar, M. N., S.: 3D printed concrete using Portland pozzolana cement-fly ash based. In: *E3S Web of Conferences* (Vol. 529, p. 01019). EDP Sciences (2024). <https://doi.org/10.1051/e3sconf/202452901019>
27. Panda, B. 3D printing of high-volume fly ash mixtures for digital concrete construction (Doctoral dissertation). <https://doi.org/10.32657/10356/93583>
28. Sahin, H. G., Mardani, A. & Mardani, N. Performance Requirements and Optimum Mix Proportion of High-Volume Fly Ash 3D Printable Concrete. In: *Buildings*, **14**(7), (2024). (2024). <https://doi.org/10.3390/buildings14072069>
29. Tao, J. L. et al. Leveraging internal curing effect of fly Ash cenosphere for alleviating autogenous shrinkage in 3D printing. *Constr. Build. Mater.* **346**, 128247. <https://doi.org/10.1016/j.conbuildmat.2022.128247> (2022).
30. Manikandan, K., Wi, K., Zhang, X., Wang, K. & Qin, H. Characterizing cement mixtures for concrete 3D printing. *Manuf. Lett.* **24**, 33–37. <https://doi.org/10.1016/j.mfglet.2020.03.002> (2020).
31. Liu, C. et al. Influence of hydroxypropyl Methylcellulose and silica fume on stability, rheological properties, and printability of 3D printing foam concrete. *Cem. Concr. Compos.* **122**. <https://doi.org/10.1016/j.cemconcomp.2021.104158> (2021).
32. Bhattacharjee, S. et al. Sustainable materials for 3D concrete printing. *Cem. Concr. Compos.* **122**, 104156. <https://doi.org/10.1016/j.cemconcomp.2021.104156> (2021).
33. Duan, Z. et al. Effect of Metakaolin on the fresh and hardened properties of 3D printed cementitious composite. *Constr. Build. Mater.* **350**, 128808. <https://doi.org/10.1016/j.conbuildmat.2022.128808> (2022).
34. Chen, M. et al. Yield stress and Thixotropy control of 3D-printed calcium sulfoaluminate cement composites with Metakaolin related to structural build-up. *Constr. Build. Mater.* **252**, 119090. <https://doi.org/10.1016/j.conbuildmat.2020.119090> (2020).
35. Chen, Y. et al. Limestone and calcined Clay-Based sustainable cementitious materials for 3D concrete printing: A fundamental study of extrudability and Early-Age strength development. *Appl. Sci.* **9** (9), 1809. <https://doi.org/10.3390/app9091809> (2019).
36. Abdalqader, A., Sonebi, M., Dedenis, M., Amziane, S. & Perrot, A. Mechanical Performance of 3-D Printed Concrete Containing Fly Ash, Metakaolin and Nanoclay. In: *RILEM International Conference on Concrete and Digital Fabrication* (pp. 111–116). Cham: Springer International Publishing, (2022).
37. Yang, H., Che, Y. & Shi, M. Influences of calcium carbonate nanoparticles on the workability and strength of 3D printing cementitious materials containing limestone powder. *J. Building Eng.* **44**, 102976. <https://doi.org/10.1016/j.jobe.2021.102976> (2021).
38. Jia, Z. et al. Printability and mechanical properties of 3D printing ultra-high performance concrete incorporating limestone powder. *Constr. Build. Mater.* **426**, 136195. <https://doi.org/10.1016/j.conbuildmat.2024.136195> (2024).
39. Kruger, J., Zeranka, S. & van Zijl, G. An Ab initio approach for Thixotropy characterization of (nanoparticle-infused) 3D printable concrete. *Constr. Build. Mater.* **224**, 372–386. <https://doi.org/10.1016/j.conbuildmat.2019.07.078> (2019).
40. Sikora, P. et al. The effects of Nanosilica on the fresh and hardened properties of 3D printable mortars. *Constr. Build. Mater.* **281**, 122574. <https://doi.org/10.1016/j.conbuildmat.2021.122574> (2021).
41. Ma, G., Li, Z. & Wang, L. Printable properties of cementitious material containing copper tailings for extrusion based 3D printing. *Constr. Build. Mater.* **162**, 613–627. <https://doi.org/10.1016/j.conbuildmat.2017.12.051> (2018).
42. Li, X. et al. Preparation and microstructural characterization of novel 3D printable Building material composed of copper tailings and iron tailings. *Constr. Build. Mater.* **249**, 118779. <https://doi.org/10.1016/j.conbuildmat.2020.118779> (2020).

43. Casagrande, C. A., Roque, J. S., Jochem, L. F., Correa, J. N. & Medeiros, A. Copper slag in cementitious composites: A systematic review. *J. Building Eng.* **78**, 107725. <https://doi.org/10.1016/j.jobee.2023.107725> (2023).
44. Olejnik, T. P., Gluba, T. & Obraniak, A. Kinetyka Mielenia Kwarcytu Przy Kaskadowym Ruchu Złoża Nadawy. In: *Inżynieria I Aparatura Chem.*, 100–101., (2009).
45. Londono-Zuluaga, D. et al. Report of RILEM TC 267-TRM phase 3: validation of the R3 reactivity test across a wide range of materials. *Mater. Struct.* **55**, 142. <https://doi.org/10.1617/s11527-022-01947-3> (2022).
46. PN-EN 196-. 1:2016-07 Methods of Testing cement - Part 1: Determination of strength.
47. PN-EN 1015-. 3 Determination of the consistency of fresh mortar (using a spreading table).
48. Roussel, N. et al. *RILEM TC PFC, Performance Requirements and Testing of Fresh Printable cement-based Materials* (slug test, 2023).
49. Edwin, R. S., Gruyaert, E. & De Belie, N. Influence of intensive vacuum mixing and heat treatment on compressive strength and microstructure of reactive powder concrete incorporating secondary copper slag as supplementary cementitious material. *Constr. Build. Mater.* **155**, 400–412 (2017).
50. Skočibušić Pejić, J., Bašić, A. D., Grubor, M. & Serdar, M. Link between the reactivity of slag and the strength development of calcium aluminate cement. *Materials* **17** (14), 3551. <https://doi.org/10.3390/ma17143551> (2024).
51. Afshoon, I. & Sharifi, Y. Use of copper slag microparticles in self-consolidating concrete. *ACI Mater. J.* **114** (5), 691–699. <https://doi.org/10.14359/51700887> (2017).
52. Adhavanathan, T. & Vinoth, V. Experimental investigation of self compacting concrete by using copper slag and fly Ash. *Int. J. Sci. Res. Dev.* **3**, 384–389 (2015).
53. Zhang, J., Wang, J., Dong, S., Yu, X. & Han, B. A review of the current progress and application of 3D printed concrete. *Compos. Part A: Appl. Sci. Manuf.* **125**, 105533. <https://doi.org/10.1016/j.compositesa.2019.105533> (2019).
54. Van Overmeir, A. L., Figueiredo, S. C., Šavija, B., Bos, F. P. & Schlangen, E. Design and analyses of printable strain hardening cementitious composites with optimized particle size distribution. *Constr. Build. Mater.* **324**, 126411. <https://doi.org/10.1016/j.conbuildmat.2022.126411> (2022).
55. Pott, U., Wolf, C., Petryna, Y. & Stephan, D. Evaluation of the unconfined uniaxial compression test to study the evolution of apparent printable mortar properties during the early age transition regime. *Cem. Concr. Res.* **161**, 106956. <https://doi.org/10.1016/j.cemconres.2022.106956> (2022).
56. Mazhoud, B., Perrot, A., Picandet, V., Rangeard, D. & Courteille, E. Underwater 3D printing of cement-based mortar. *Constr. Build. Mater.* **214**, 458–446. <https://doi.org/10.1016/j.conbuildmat.2019.04.134> (2019).
57. Suiker, A. S. J. Mechanical performance of wall structures in 3D printing processes: theory, design tools and experiments. *Int. J. Mech. Sci.* **137**, 145–170. <https://doi.org/10.1016/j.ijmecsci.2018.01.010> (2018).
58. Józwiak-Niedźwiedzka, D. Microscopic observations of self-healing products in calcareous fly Ash mortars. *Microsc. Res. Tech.* **78** (1), 22–29. <https://doi.org/10.1002/jemt.22440> (2015).
59. Zain, M. F. M., Islam, M. N., Radin, S. S. & Yap, S. G. Cement-based solidification for the safe disposal of blasted copper slag. *Cem. Concr. Compos.* **26** (7), 845–851. <https://doi.org/10.1016/j.cemconcomp.2003.08.002> (2004).
60. Potysz, A. et al. Copper metallurgical slags—current knowledge and fate: a review. *Crit. Rev. Environ. Sci. Technol.* **45** (22), 2424–2488. <https://doi.org/10.1080/10643389.2015.1046769> (2015).

Author contributions

MN - writing an original text and conduct of research AC, BS - research coordination MN, AC, BS - all checked the manuscript.

Declarations

Competing interests

The authors declare no competing interests.

Additional information

Correspondence and requests for materials should be addressed to M.N.

Reprints and permissions information is available at www.nature.com/reprints.

Publisher's note Springer Nature remains neutral with regard to jurisdictional claims in published maps and institutional affiliations.

Open Access This article is licensed under a Creative Commons Attribution-NonCommercial-NoDerivatives 4.0 International License, which permits any non-commercial use, sharing, distribution and reproduction in any medium or format, as long as you give appropriate credit to the original author(s) and the source, provide a link to the Creative Commons licence, and indicate if you modified the licensed material. You do not have permission under this licence to share adapted material derived from this article or parts of it. The images or other third party material in this article are included in the article's Creative Commons licence, unless indicated otherwise in a credit line to the material. If material is not included in the article's Creative Commons licence and your intended use is not permitted by statutory regulation or exceeds the permitted use, you will need to obtain permission directly from the copyright holder. To view a copy of this licence, visit <http://creativecommons.org/licenses/by-nc-nd/4.0/>.

© The Author(s) 2025